DOI 10.1007/s10511-015-9373-x
Astrophysics, Vol. 58, No. 2, June, 2015

ENVIRONMENTAL DENSITY vs. COLOUR INDICES OF THE LOW REDSHIFTS GALAXIES

D. V. Dobrycheva,[1] O. V. Melnyk,[2] I. B. Vavilova,[1] and A. A. Elyiv[1,3]

We have used 3D Voronoi tessellation to determine the environmental density of galaxies from a sample of the SDSS DR9 survey ($0.02 < z < 0.1$ and $m_r < 17.7$). The sample was divided into two groups: bright central galaxies with $M_r < -20.7$ ($N \sim 120000$) and faint satellite galaxies with $M_r > -20.7$ ($N \sim 140000$). We characterized the environmental density of the galaxies by the inverse volume of a Voronoi cell. We confirmed a tendency for an evolutionary decrease in the relative number of early galaxy types (with quenched star formation) with increasing redshift. It was also shown that the higher the density of environment near a central galaxy, it is more likely that the central galaxy has an early morphological type. The fraction of early types among the central galaxies is higher (78%) that among the sample of satellite galaxies (26%). In addition, the higher fraction of the central early-type galaxies in the sample, the higher their share in the denser environments.

Keywords: *galaxies: environmental density: morphology: colour indices: SDSS galaxies: Voronoi tessellation*

(1) Main Astronomical Observatory, National Academy of Sciences of Ukraine, Ukraine; e-mail: daria@mao.kiev.ua, irivav@mao.kiev.ua
(2) Astronomical Observatory, National Taras Shevchenko University of Kyiv, Ukraine; e-mail: melnykol@gmail.com
(3) Department of Physics and Astronomy, University of Bologna, Italy; e-mail: andrii.elyiv@gmail.com

Original article submitted December 18, 2014; accepted for publication April 10, 2015. Translated from Astrofizika, Vol. 58, No. 2, pp. 183-196 (May 2015).

1. Introduction

The morphology of galaxies, as well as their luminosity, colour, mass, and star formation rate, depends on their environments: in regions with a high concentration of galaxies the fraction of galaxies of early types is considerably higher than in less populated regions [1-3]. Spiral galaxies with a high star formation rate avoid densely populated cluster regions [4-9]. Here, the influence of surroundings is such that spiral galaxies in clusters have the earlier types than the spiral galaxies in the field [10,11], while their reserves of neutral hydrogen are lower [12]. Galaxies in voids are generally of a later type and have a higher gas content per unit luminosity than galaxies in groups and clusters [13]. The star formation rate in the centers of disc galaxies in clusters is higher than in the of the same type field galaxies, and the galaxies in clusters exhibit clear signs of perturbations [14]. It has been shown [15] that the evolutionary transformation in the morphology of galaxies from later to earlier types are usually accompanied by a change in their colour toward the red, but a transformation in the colour of a galaxy does not always trigger a fundamental modification of its morphological type [16]. The evolution of bimodality has also been observed in the colour distribution of galaxies: the fraction of red massive galaxies in the current epoch ($z \sim 0$) is substantially higher than in earlier epochs [17-19].

An interrelation between the properties of galaxies and the density of their surroundings shows up at the scales of low-population groups, pairs, and triplets of galaxies, as well as in the scales of clusters. It has been shown by Karachentsev [20] and in a series of our papers [21-24] that the fraction of galaxies of early types in pairs and triplets is higher than in isolated galaxies. Here it is interesting that the optical (g-r) and near infrared (J-H) colors of early type galaxies are independent on the environmental density, while spiral and late type galaxies are considerably redder in pairs and triplets than isolated galaxies. The exception is galaxies in very close pairs (with signs of interactions); they are somewhat bluer than isolated galaxies.

The mechanism of star formation quenching in galaxies is currently under discussion: why do spiral galaxies lose gas as they evolve into red elliptical/lenticular systems at $z < 2$? What do physical processes cause a change in the colour indices of galaxies from blue to red: internal causes owing to the galactic mass, including the presence of active galactic nuclei (AGN) and/or their surroundings, and how are these external and internal factors related [26-29]? It appears that galaxies with large masses have a red colour independently on their surroundings and morphology. Less massive galaxies are usually bluer and are in less dense surroundings, and they become redder as the environmental density is increases, regardless of their morphological type [30,31]. So the mass of a galaxy is the major factor in the evolution of central (more massive) galaxies, while the properties of satellite galaxies depend strongly on the influence of the surroundings. The “influence of the surroundings” is taken to mean the interaction and merging of galaxies, and a strangulation by which gas is blown out of a galaxy due to the gravitational field of a cluster. The shape of a central galaxy can also change as a result of gravitational interactions with smaller satellite galaxies, as well as through ram pressure stripping that can remove cold gas from galaxies owing to high velocity motions within a cluster [32-34]. The environmental density also determines trends of clustering of satellite galaxies. For example, a study of low surface brightness (LSB) dwarf galaxies in the volume of the Local Supercluster has shown that these galaxies, both the ones enriched in gas (dIr, dIm) and those with a low gas content (dSph), have the same

tendency to clustering together in the field of the supercluster [35,36]. In regions of high density (the clusters in Virgo and Fornax), the LSB dwarf galaxies are of later types (dSm, dIr, dIm) and bright spiral galaxies avoid the centers of the clusters, while the density of the distribution of dwarf (dE, dSph) and normal galaxies (E-S0) of early types is well described by the King profile, and the linear dimensions of the dE-Sph satellite galaxies are independent of the environmental density [37,38]. The fraction of early satellite galaxies is higher in the halo of a central galaxy of an earlier type than in the halo of a central galaxy of a later type with the same mass [3]. The correlation between the properties of a central galaxy and the satellite galaxies is still an open questions, since previous work on this topic give a contradictory conclusions [39,23].

This paper is a study of the effect of environment on the colour indices (morphology) of galaxies, as well as on the evolution of bimodality in their colour indices at low redshifts ($z < 0.1$), based on a large sample of galaxies from the Sloan Digital Sky Survey 9th release (SDSS DR9). We use the Voronoi tessellation method to determine the relative spatial density of the galaxies. It is well recommended for the study of large-scale structure and for isolating groups and clusters of galaxies [21,40-44].

2. The sample

The procedure for compiling the sample is described in detail elsewhere [45]. Here we limit ourselves to describing the key stages in selecting the galaxies for the sample and the main characteristics of the sample.

The original sample from the SDSS DR9 was consisted of 724 thousand objects with $z < 0.1$. After stars and duplicates were eliminated from the sample and the sample was restricted to redshifts and visual magnitudes of

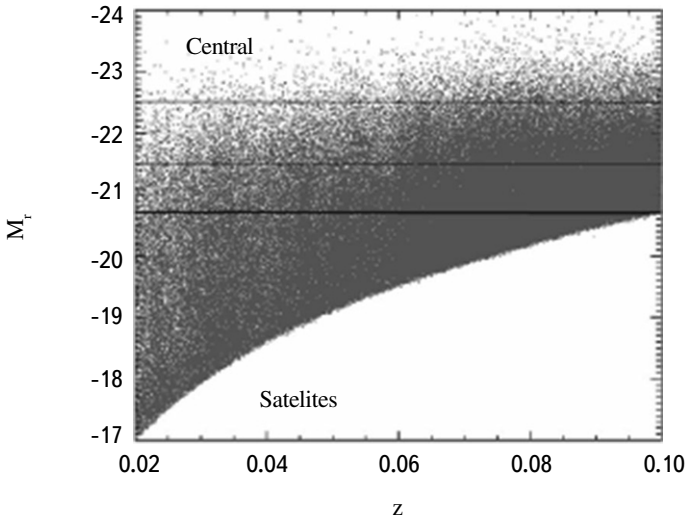

Fig. 1. The absolute magnitude of galaxies as a function of red shift for central galaxies and their faint satellites.

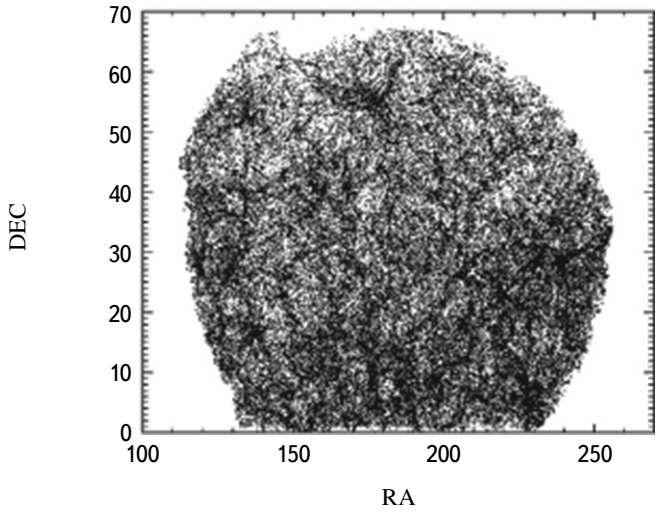

Fig. 2. The distribution of central galaxies with $M_r < -20.7$ over the sky in equatorial coordinates.

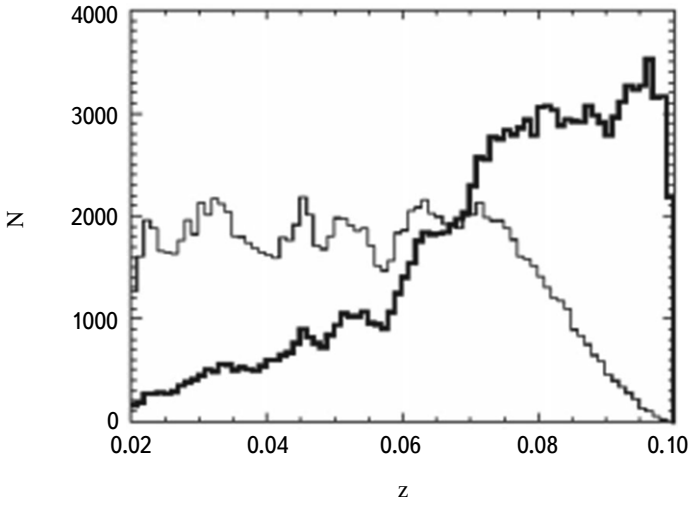

Fig. 3. The distributions of the central galaxies (bold curve) and satellite galaxies (thin curve) with respect to red shift.

$0.02 < z < 0.1$ and $m_r < 17.7$, respectively, 260000 galaxies were remained. In order to use Voronoi tessellation, the sample must be as uniform as possible. Thus, we began by applying the Voronoi tessellation to a sample of bright central galaxies with $M_r < -20.7$ ($N \sim 120000$) and then examined the properties of the environments of central galaxies consisting of their fainter satellites, galaxies with $M_r > -20.7$ ($N \sim 140000$). Figure 1 shows the dependence of absolute magnitude on redshift for the bright central galaxy and their weaker satellites in the studied sample. The absolute magnitude

$$M_r = m_r - 5\log(V/H_0) - 25 - K(z) - \text{ext}$$

was corrected for Galactic absorption *ext* in accordance with [46] and a *K* - correction *K*(*z*) according to [47 - 48]. Here we used the CDM model of the Universe with the WMPS7 cosmological parameters ($\Omega_M = 0.27$, $\Omega_\Lambda = 0.73$, $\Omega_k = 0$, $H_0 = 0.71$) [34].

After applying the Voronoi tessellation (see the next section) to the sample of central galaxies, we eliminated the edge galaxies in the sample since the Voronoi tessellation is sensitive to edge effects. The distribution of the central galaxies over the sky is shown in Fig. 2, and the corresponding distributions of the central galaxies and their fainter satellites with respect to redshift are shown in Fig. 3. It can be seen that the number of central galaxies at z = 0.07 is comparable to the number of satellites because of the decrease of number of faint galaxies with redshift.

3. Voronoi tessellation

In order to apply the Voronoi mosaic (tessellation) method we have done transition from equatorial coordinates and velocities to the comoving *x, y, z* coordinates for each central galaxy in our sample (M_r < -20.7). To do this we transformed the redshift z to the corresponding distance $\chi(z)$ for each galaxy by integrating as

$$\chi(z) = D_H \int_0^z \frac{dz'}{E(z')},$$

where $D_H = c/H_0$ is the Hubble distance and $E(z')$ is the Hubble parameter, defined as

$$E(z') = \sqrt{\Omega_M (1+z)^3 + \Omega_k (1+z)^2 + \Omega_\Lambda}\ .$$

The coordinates *x, y, z* of the galaxies in the comoving space are determined as

$$x = \chi(z)\cos(\theta)\cos(\varphi),$$

where θ is the declination of each galaxy, φ is the right ascension, and $\chi(z)$ is the corresponding distance for redshift *z*.

After getting the three dimensional cartesian coordinates of the galaxies, we divided the geometrical space occupied by the galaxy sample in mosaic cells (volumes *V* in the 3D case). Each cell has a galaxy as nucleus and consists of elementary volumes of space closer to this galaxy than to any other galaxy [49,50]. The use of the Voronoi tessellation to isolate groups of galaxies in three dimensions has been described in detail by Melnyk et al. [51]. Figure 4 shows an example of the Voronoi tessellation in a two dimensional case to make it easier to see. Figure 5 shows the distribution of the inverse volumes (1/*V*) of the Voronoi cells for the sample of central galaxies. We shall use

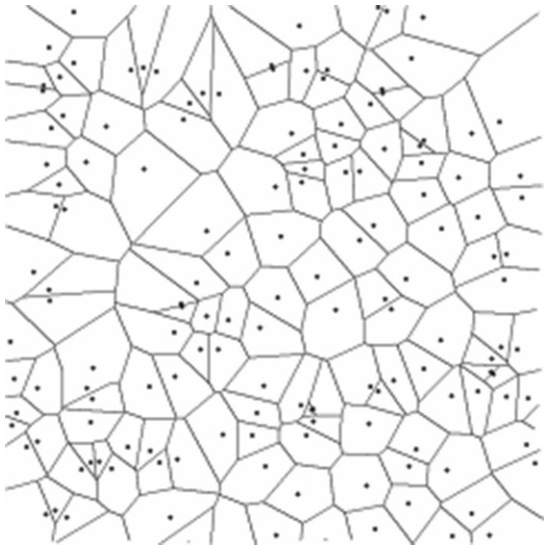

Fig. 4. An example of the construction of 2D Voronoi tessellation.

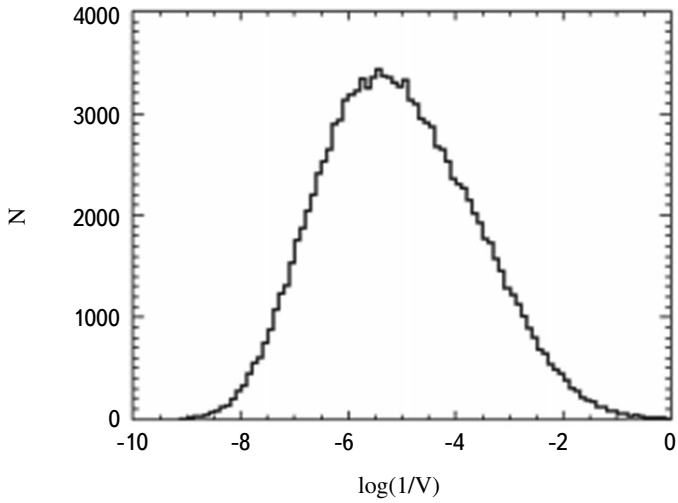

Fig. 5. The quantitative distribution of the inverse volumes $1/V$ of Voronoi cells for the central galaxies with M_r <- 20.7.

this value in the following to describe the density of galaxy environments; when $1/V$ is higher, a galaxy is less isolated.

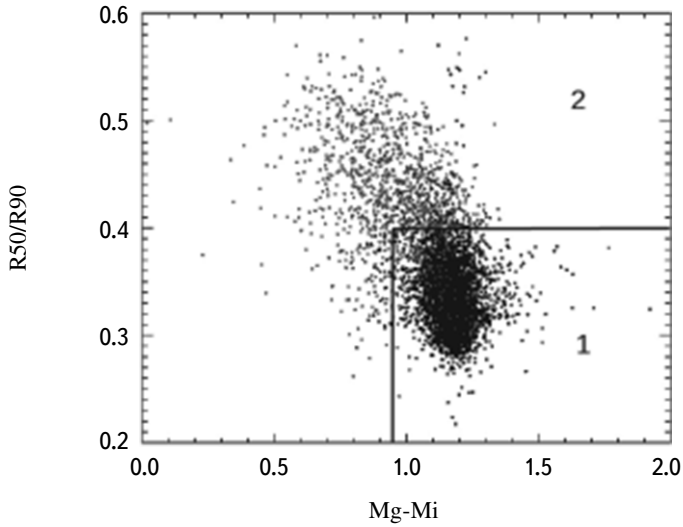

Fig. 6. Inverse concentration indices as a function of color indices for the 5000 bright galaxies in the sample with the lowest Voronoi cell volumes. The black and grey points indicate visually classified galaxies of types E-S0 and, Sa-Irr types respectively. Most of the galaxies of these types are in the corresponding regions 1 and 2 (in accordance with the criterion we proposed in [23]).

4. Results

Since the colour indices and the concentration indices toward the center of a galaxy correlate with its morphological type, it is convenient to classify a large sample by morphological types by using only these parameters [52,53]. We have applied a similar approach previously [23,54,55] and showed that visual and "automatic" morphological classification using the colour indices and the inverse concentration indices $R50/R90$ satisfy the for the overwhelming majority (over 80%) of the galaxies in the sample.

In this paper we carried out visual classification of the 5000 central galaxies with the smallest Voronoi cell volumes (i.e., the largest values of $1/V$ [55]). Figure 6 shows $R50/R90$ as a function of the colour indices g-i for galaxies of the early E-S0 and late Sa-Irr morphological types. Regions 1 and 2 correspond to the criteria obtained by Melnyk et al. [23] for classification of the galaxies: specifically, $0.95 < g-i < 1.5$ and $0 < R50/R90 < 0.4$ for the E+S0 types; ($0 < g-i < 0.95$ and $0 < R50/R90 < 0.6$) and ($0.95 < g-i < 1.5$ and $0.4 < R50/R90 < 0.6$) for the S+Irr types of galaxies. Table 1 lists the percent estimates of agreement (coincidence) of the combined types in a test sample of 5000 central galaxies in "their" regions 1 and 2. Thus, about 95% of the E+S0 galaxies lie in region 1 and 78% of the Sa-Irr lie in region 2. This indicates that the chosen criterion provides a good description of the morphological types of the test sample. Note that here the galaxies have larger redshifts than in [23]. An extrapolation of these criteria to the entire sample of central galaxies is shown in Fig. 7. Here 61% of galaxies (N = 75973) of the sample

TABLE 1. Fraction of Visually Determined Morphological Types E-S0 and Sa-Irr in Regions 1 and 2 (see Fig. 7) for the 5000 Bright Galaxies with the Smallest Voronoi Cell Volumes. Regions 1 and 2 are Defined According to the Values of the Color Indices *Mg-Mi* and of the Inverse Concentration Indices *R*50/*R*90

Sample	*N*	Region 1 (E-S0), %	Region 2 (Sa-Irr), %
N-S0	3876	95.1	4.9
Sa-Irr	1124	21.6	78.4

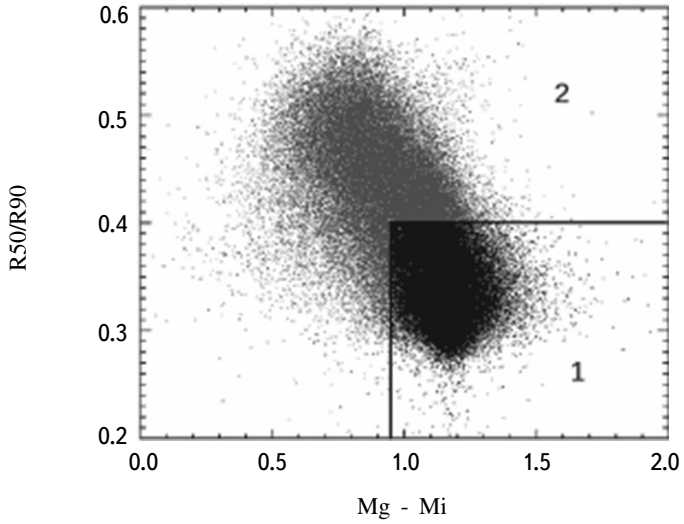

Fig. 7. Reciprocal concentration index as a function of color indicies for the central bright galaxies of the sample. The lines indicate the galaxies in regions 1 and 2 that correspond to morphological types E-S0 and Sa-Irr according to our criterion (see Fig. 6).

lie in region 1 (early E+S0 types) and 39% (N = 48248) in region 2 (late Sa-Scd types). For the satellite galaxies the percentages are 26% and 74%, respectively. Here we note that the test sample of 5000 central galaxies with minimum volumes contained 78% and 22% of E-S0 and Sa-Irr type galaxies, respectively. These statistical estimates indicate that when a galaxy is of an earlier type, it lies in a denser environment and that when a galaxy is brighter (i.e., more massive), it is of an earlier type. The sample of central bright galaxies contains a fairly high number of early E + S0 galaxies (because of the limitation to $M_r < -20.7$) , which reduces the amount of late Sa-Irr galaxies in the sample. In the rest of this paper we use the criteria for morphological classification employed in [23], which is illustrated in Figs. 6 and 7, i.e., we refer to the galaxies lying in regions 1 and 2, respectively, as early E-S0 and

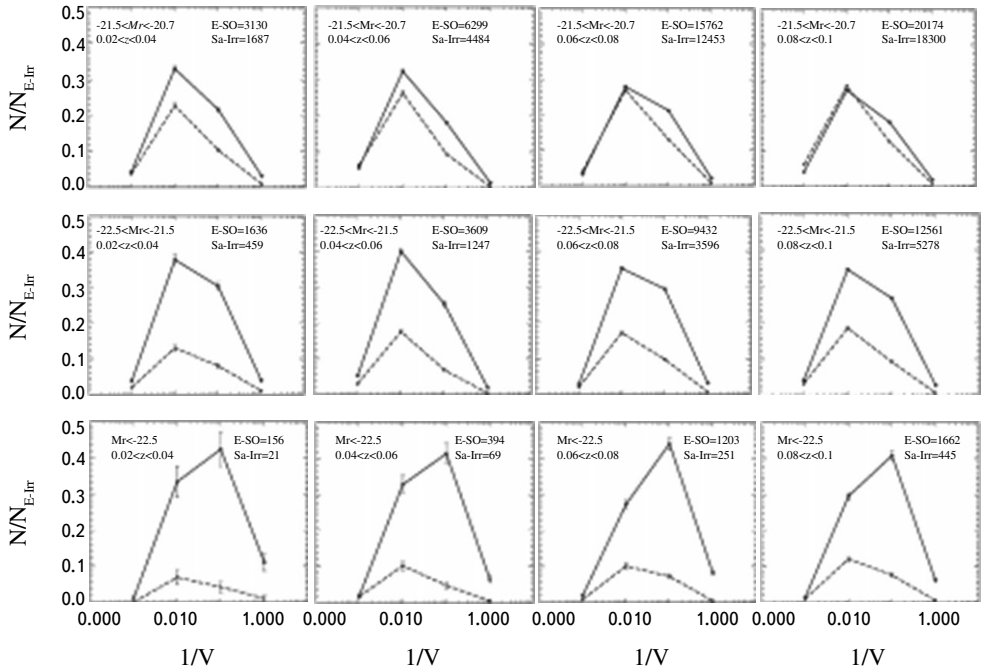

Fig. 8. The distribution of the number of galaxies with respect to the inverse volume of the Voronoi cells, with E-S0 indicated by solid lines and Sa-Irr indicated by dashed lines, for different ranges of red shift and luminosity. The number of galaxies in each bin is normalized to the total number of E-Irr within the given subsample. The number of central bright E-S0 and Sa-Irr galaxies is shown in each frame.

late Sa-Irr.

Figure 8 shows the distributions of E-S0 and Sa-Irr galaxies with respect to the reciprocal volume of the Voronoi cells that contain them. The cells have been grouped into 4 logarithmic intervals $1/V < 0.001$, $0.001 < 1/V < 0.01$, $0.01 < 1/V < 0.1$, and $1/V > 0.1$ for four ranges of the redshift $0.02 < z < 0.04$, $0.04 < z < 0.06$, $0.06 < z < 0.08$, and $0.08 < z < 0.1$ (in the rows) and for different ranges of absolute stellar magnitude, $-21.5 < M_r < -20.7$, $-22.5 < M_r < -21.5$, and $M_r < -22.5$ (in the columns). The number of galaxies in each bin for the E-S0 and Sa-Irr types is normalized to the total number of E-Irr galaxies within the given subsample and is indicated in each of the frames. Figure 8 shows that the fraction of galaxies of spiral and late types becomes larger while redshift increasing, while the fraction of early types, on the contrary, is smaller. That follows the well known evolutionary trend of a reduction in the number of galaxies with suppression of star formation for increasing redshift [18,41,19], even at comparatively low redshifts down to $z < 0.1$. In addition, for the brighter galaxies in the sample, the fraction of galaxies of earlier types is larger since, on the average, earlier types have higher luminosities (the well known type/colour indices-luminosity relation) [2,56,57]. The brightest galaxies of earlier types with $M_r < -22.5$ appear preferentially in denser environments: the peak of the distribution of the inverse volumes of the Voronoi cells for the E-S0 types lie within the interval $0.01 < 1/V < 0.1$, while in other intervals of M_r, for the Sa-Irr types the peak of the distribution always is within $0.001 < 1/V < 0.01$ (the morphology-density relation [1,2,23,31,57]).

We also have determined the density of galaxies in a Voronoi cell including their faint satellites, i.e., galaxies

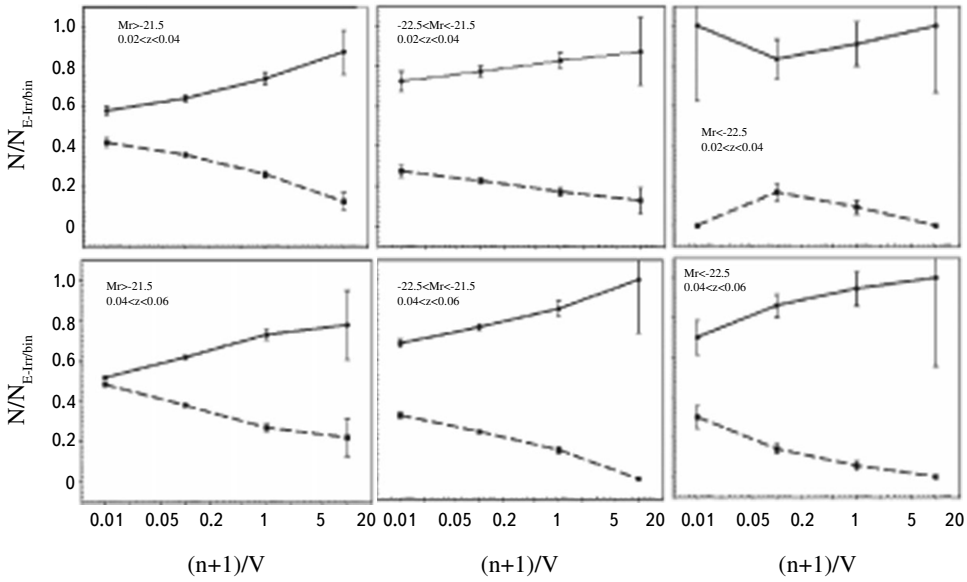

Fig. 9. The distribution of the number of galaxies with respect to the density of galaxies in the Voronoi cells, $(n+1)/V$, where n is the number of faint galaxies with $Mr > -20.7$ and V is the volume of the Voronoi cell, for different ranges of red shifts and luminosities. The types E-S0 (solid line) and Sa-Irr (dashed line) correspond to central galaxies which are the nuclei of the corresponding Voronoi cells. The number of galaxies in each bin is normalized to the total number of central E-Irr galaxies within a given bin, $(n+1)/V$.

with $M_r > -20.7$: $(n + 1)/V$, where n is the number of faint galaxies in the Voronoi cell and V is the volume of the Voronoi cell. Figure 9 shows the distributions of early E+S0 (smooth curves) and Sa-Irr types (dashed curves) with respect to the parameter $(n + 1)/V$ in four intervals: $(n + 1)/V < 0.01$, $0.01 < (n + 1)/V < 0.1$, $0.1 < (n + 1)/V < 1$, and $(n + 1)/V > 1$. The number of galaxies is normalized to the number of E-Irr galaxies within the given range of $(n + 1)/V$. We examined the density of galaxies only in the first two redshift intervals, since we cannot evaluate the evolution of their properties at higher z because there are not enough faint galaxies (see Fig. 3). We can, however, compare the environmental density of the galaxies as a function of the absolute magnitude and morphological type of the central bright galaxy. Thus, as Fig. 9 shows, the fraction of early types of central galaxies increases with increasing environmental density, while, on the other hand, the fraction of late types decreases; that is, the earlier types are in a denser environment than the late types. When the central galaxy is brighter the fraction of early types in a subsample will be larger.

5. Conclusions

3D Voronoi tessellation has been applied to the sample of galaxies [45] based on the SDSS DR9 survey ($0.02 < z < 0.1$ and $m_r < 17.7$) to determine the environmental density of the galaxies. The galaxies in the sample

were divided into two groups: bright central galaxies with $M_r < -20.7$ ($N \sim 120000$) and faint satellite-galaxies with $M_r > -20.7$ ($N \sim 140000$). In order to avoid selection effects, the Voronoi tessellation was applied to the sample of central galaxies. We characterized the environmental density of galaxies by the inverse volume $1/V$ of the Voronoi cell. The major conclusions are the follows:

1. At comparatively low redshifts $z < 0.1$, the evolutionary trend of a reduction in early galaxy types (with quenched star formation) with increasing redshift is followed. Thus, the fraction of early types decreases with redshift while, on the contrary, the fraction of spirals and late types increases.

These results are consistent with data from other authors [17,18,41,19] showing that the fraction of red massive galaxies in the current epoch ($z \sim 0$) is considerably larger than in earlier epochs.

2. When the environmental density of the central galaxies is higher (i.e., when $1/V$ is lower), it is more probable that the central galaxies are of an early type. In addition, as the density of faint galaxies environment a bright central galaxy increases, the fraction of central galaxies of early types increases, while that of the late types decreases.

This conclusion is in accord with the classical morphology-density relation by which the fraction of early type galaxies is considerably larger in clusters than in the field. This relation is confirmed in works by other authors who examined another samples of galaxies and different indicators of their environmental densities [2,18,23,31,57, and the papers on samples of galaxies from the Local supercluster cited in the *Introduction*].

3. The brighter the galaxies in the sample, the fraction of central early type galaxies is higher, and their fraction in a denser environment is higher. In addition, the fraction of galaxies of early types among the bright central galaxies is higher (78%) than in a sample of satellite-galaxies (26%). This is explained by the fact that, on the average, galaxies of early types have higher luminosity, thereby confirming that galaxies with higher luminosity are in denser environments than less bright galaxies [2,3,34,56-58].

It has been shown [15,19,27,28,31] that central galaxies and satellite-galaxies evolve in different ways while, on the contrary, correlations have been found [3,39] between the properties of central galaxies and their satellites, which must indicate that they evolve together. Thus, in our next paper we plan to analyze correlations between the colour indices and other properties of the central galaxies and the satellite galaxies (including dwarf LSB galaxies) in the sample studied here.

We thank the scientific group working on the Sloan Digital Sky Survey http://www.sdss3.org. Funding from SDSS-III has been provided by the Alfred P. Sloan Foundation and the U.S. Dept. of Energy Office of Science. This work was done as part of project No. 299Ts “Study of the physical properties of galaxies in the Local Universe” of the Main Astrophysical Observatory of the National Academy of Sciences of Ukraine.

REFERENCES

1. A. Dressler, Astrophys. J. **236**, 351 (1980).
2. M. R. Blanton, D. Eisenstein, D. W. Hogg, et al., Astrophys. J. **629**, 143 (2005).

3. S. M. Weinmann, F. C. van den Bosch, X Yang, et al., Mon. Not. Roy. Astron. Soc. **366**, 2 (2006).
4. Y. Hashimoto, A. Oemler Jr., and H. Lin, Astrophys. J. **499**, 589 (1998).
5. I. Lewis, M. Balogh, R. de Propris, et al., Mon. Not. Roy. Astron. Soc. **334**, 673 (2002).
6. P. Gomez, R. C. Nichol, C. J. Miller, et al., Astrophys. J. **584**, 210 (2003).
7. M. Balogh, V. Eke, G. Miller., et al., Mon. Not. Roy. Astron. Soc. **348**, 1355 (2004).
8. H. J. Martinez, A. Zandivarez, M. Domingues, et al., Mon. Not. Roy. Astron. Soc. **333**, 31 (2002).
9. P. Serro, T. Dosterloo, R. Morganti, et al., Mon. Not. Roy. Astron. Soc. **422**, 1835 (2012).
10. R. C. Kennicutt Jr., Astron. J. **88**, 483 (1983).
11. J. M. Gabor and R. Dove, arXiv:1405.1043 (2014).
12. G. Gavazzi, K. O'Neil, A. Boselli, and W. van Driel, Astron. Astrophys. **449**, 929 (2006).
13. A. A. Elyiv, L. D. Karachentsev, V. E. Karachentseva, et al., Astrophys. Bull. **68**, 1 (2013).
14. C. F. Bretherton, C. Moss, and P. A. James, Astron. Astrophys. **553**, 67 (2013).
15. R. A. Skibba, S. P. Bamford, R. C. Nichol, et al., Mon. Not. Roy. Astron. Soc. **399**, 966 (2009).
16. K. Schawinski, C. M. Urry, B. D. Simmons, et al., Mon. Not. Roy. Astron. Soc. **440**, 889 (2014).
17. I. K. Baldry, K. Glazebrook, J. Brinkmann, et al., Astrophys. J. **600**, 681 (2004).
18. O. Cucciati, A. Iovino, C. Marinoni, et al., Astron. Astrophys. **458**, 39 (2006).
19. T. Tal, A. Dekel, P. Oesch, et al., Astrophys. J. **789**, 11 (2014).
20. I. D. Karachentsev, Binary Stars [in Russian], Nauka, Moscow (1987), 248 pp.
21. O. V. Mel'nik, Pis'ma v Astron. zh. **32**, 338 (2006).
22. I. B. Vavilova, O. V. Melnyk, and A. A. Elyiv, Astron. Nachr. **330**, 1004 (2009).
23. O. V. Melnyk, D. V. Dobrycheva, and I. B. Vavilova, Astrophysics, **55**, 293 (2012).
24. O. Melnyk, S. Mitronova, and V. E. Karachentseva, Mon. Not. Roy. Astron. Soc. **438**, 548 (2014).
25. M. Fernandez Lorenzo, J. Sulentic, L. Verdes-Montenegro, et al., Astron. Astrophys. **540**, A47 (2012).
26. G. Kauffmann, S. D. M White, T. M. Heckman, et al., Mon. Not. Roy. Astron. Soc. **353**, 713 (2004).
27. J. L. Tinker, A. Leauthaud, K. Bundy, et al., Astrophys. J. **778**, 18 (2013).
28. K. Kuvac, S. J. Lilly, C. Knobel, et al., Mon. Not. Roy. Astron. Soc. **438**, 717 (2014).
29. A. R. Wetzel, J. L. Tinker, C. Conroy, et al., Mon. Not. Roy. Astron. Soc. **439**, 2687 (2014).
30. S. P. Bamford, R. C. Nichol, I. K. Baldry, et al., Mon. Not. Roy. Astron. Soc. **393**, 1324 (2009).
31. Y.-J. Peng, S. J. Lilly, K. Kovac, et al., Astrophys. J. **721**, 193 (2010).
32. I. K. Baldry, M. L. Balogh, R. G. Bower, et al., Mon. Not. Roy. Astron. Soc. **373**, 469 (2006).
33. A. Boselli and G. Gavazzi, Publ. Astron. Soc. Pacif. **118**, 517 (2006).
34. F. C. van den Bosch, D. Aquino, X. Yanget, et al., Mon. Not. Roy. Astron. Soc. **387**, 79 (2008).
35. V. E. Karachentseva and I. B. Vavilova, Bulletin of the Special Astrophysical Observatory, **37**, 98 (1994).
36. V. E. Karachentseva, I. B. Vavilova, ESO Conference and Workshop Proceedings **49**, 91 (1994
37. V. E. Karachentseva, I. B. Vavilova, Kinematics Phys. Ce1est. Bodies **11**, 38 (1995).
38. V. E. Karachentseva, I. B. Vavilova, Kinematics Phys. Ce1est. Bodies **11**, 49 (1995).

39. W. G. Hartley, C. J. Conselice, A. Mortlock, et al., arXiv:1406.6058 (2014).
40. A. Elyiv, O. Melnyk, and I. Vavilova, Mon. Not. Roy. Astron. Soc. **394**, 1409 (2009).
41. N. Scoville, S. Arnouts, H. Aussel, et al., Astrophys. J. Suppl. **206**, 3 (2013).
42. R. Kim, M. Strauss, N. Bahcall, et al., ASP Conference Ser. **200**, 422 (2000).
43. M. Ramella, W. Boschin, D. Fadda, et al., Astron. Astrophys. **368**, 776 (2001).
44. Marcelle Soares-Santos and Reinaldo R. de Carvalho, Astrophys. J. **727**, 45 (2011).
45. D. V. Dobrycheva, Odessa Astron. Publ. **26**, 187 (2013).
46. D. J. Schlegel, D. P. Funkbeiner, and M. Davis, Astrophys. J. **500**, 525 (1998).
47. I. Chilingarian, A.-L. Melchior, and I. Zolotukhin, Mon. Not. Roy. Astron. Soc. **405**, 1409 (2010).
48. I. Chilingarian and I. Zolotukhin, Mon. Not. Roy. Astron. Soc. **419**, 1727 (2012).
49. T. Matsuda and E. Shima, Progress of Theor. Phys. **71**, 855 (1984).
50. R. Lindenbergh, PhD Thesis (2002).
51. O. Melnyk, A. Elyiv, and I. Vavilova, Kinemat. Fiz. Nebesn. Tel **22**, 283 (2006).
52. T. Goto, C. Yamauchi, Y. Fujita, et al., Mon. Not. Roy. Astron. Soc. **346**, 601 (2003).
53. C. Park and Y.-Y. Choi, Astrophys. J. **635**, 29 (2005).
54. D. Dobrycheva and O. Melnyk, Advances in Astron. Space Phys. **2**, 42 (2012).
55. D. Dobrycheva, O. Melnyk, A. Elyiv, et al., Proceedings IAU Symposium 308 (in press).
56. I. E. Segal, Astron. Soc. Japan, Publ. (ISSN 0004-6264) **37**, 499 (1985).
57. C. Park, Y.-Y. Choi, M. S. Vogeley, et al., Astrophys. J. **658**, 898 (2007).
58. D. W. Hogg, M. R. Blanton, J. Brinkmann, et al., Astrophys. J. **601**, L29 (2004).